Khonsari et al., ***BioImpacts,*** 2022, 12(1), 21-32
doi: 10.34172/bi.2021.23389
http://bi.tbzmed.ac.ir/

Brain targeted delivery of rapamycin using transferrin decorated nanostructured lipid carriers

Fatemeh Khonsari[1], Mostafa Heydari[2], Rassoul Dinarvand[3], Mohammad Sharifzadeh[4], Fatemeh Atyabi[1,2,3*]

[1]Department of Pharmaceutics, Faculty of Pharmacy, Tehran University of Medical Sciences, Tehran, Iran
[2]Department of Pharmaceutical Nanotechnology, Faculty of pharmacy, Tehran University of Medical Sciences, Tehran, Iran
[3]Nanotechnology Research Centre, Faculty of Pharmacy, Tehran University of Medical Sciences, Tehran, Iran
[4]Department of Pharmacology and Toxicology, Faculty of Pharmacy, Tehran University of Medical Sciences, Tehran Iran

Article Info

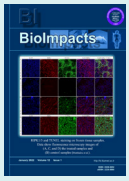

Article Type:
Original Article

Article History:
Received: 28 Aug. 2020
Revised: 8 Feb. 2021
Accepted: 18 Apr. 2021
ePublished: 9 Oct. 2021

Keywords:
Rapamycin
Nanostructured lipid carrier
Transferrin
Brain delivery

Abstract

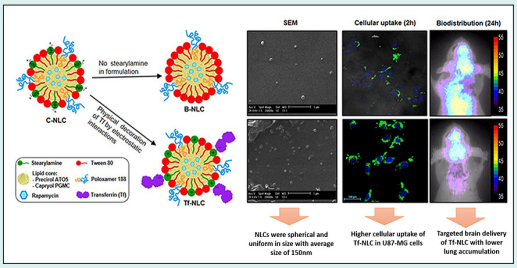

Introduction: Recent studies showed that rapamycin, as a mammalian target of rapamycin (mTOR) inhibitor, could have beneficial therapeutic effects for the central nervous system (CNS) related diseases. However, the immunosuppressive effect of rapamycin as an adverse effect, the low water solubility, and the rapid in vivo degradation along with the blood-brain barrier-related challenges restricted the clinical use of this drug for brain diseases. To overcome these drawbacks, a transferrin (Tf) decorated nanostructured lipid carrier (NLC) containing rapamycin was designed and developed.

Methods: Rapamycin-loaded cationic and bare NLCs were prepared using solvent diffusion and sonication method and well characterized. The optimum cationic NLCs were physically decorated with Tf. For *in vitro* study, the MTT assay and intracellular uptake of nanoparticles on U-87 MG glioblastoma cells were assessed. The animal biodistribution of nanoparticles was evaluated by fluorescent optical imaging. Finally, the *in vivo* effect of NLCs on the immune system was also studied.

Results: Spherical NLCs with small particle sizes ranging from 120 to 150 nm and high entrapment efficiency of more than 90%, showed ≥80% cell viability. More importantly, Tf-decorated NLCs in comparison with bare NLCs, showed a significantly higher cellular uptake (97% vs 60%) after 2 hours incubation and further an appropriate brain accumulation with lower uptake in untargeted tissue in mice. Surprisingly, rapamycin-loaded NLCs exhibited no immunosuppressive effect.

Conclusion: Our findings proposed that the designed Tf-decorated NLCs could be considered as a safe and efficient carrier for targeted brain delivery of rapamycin which may have an important value in the clinic for the treatment of neurological disorders.

Introduction

Brain drug delivery has always been one of the most challenging delivery approaches since the presence of the blood-brain barrier (BBB), as a non-fenestrated microvascular endothelial cell, restricts the transition of substances and drug molecules from the systemic circulation to the brain.[1] Limited BBB permeability of drugs decreases the therapeutic concentration in the brain and loses the therapeutic effectiveness in neurological disorders.

To bypass this barrier various strategies have been introduced to increase drug delivery into the central nervous system (CNS) including direct injection in the brain, brain implants, chemical modification of drugs, biological changes, and particulate systems.[2,3] In this manner, the use of nanoparticles offers rapid progress to the development of new plans for targeted CNS delivery. These delivery systems are able to maximize the brain's effective concentration, decrease the adverse effects and increase drug stability.[4-7]

Rapamycin or sirolimus, an immunosuppressive drug, is a large carboxylic lactone-lactam macrolide which first isolated from actinobacteria (*Streptomyces hygroscopic*) in 1975. Rapamycin by making a complex with the 12- kDa

*Corresponding author: Fatemeh Atyabi, Email: atyabifa@tums.ac.ir

FK506-binding protein (FKBP12) inhibits the mammalian target of rapamycin (mTOR), mainly mTOR complex1 (mTORC1), and thereby could regulate cell growth, proliferation, metabolism, and survival. Dysregulation of mTORC1 in neurological disorders, mainly brain tumors and neurodegenerative disease, has made rapamycin an appropriate candidate for treatment.[8,9] Iorio et al showed the effectiveness of combined treatment of rapamycin and doxorubicin in an *in vitro* and *in vivo* model of glioblastoma.[10] Spilman et al also showed the inhibition of mTOR by rapamycin could abolish the cognitive deficit and memory loss in an *in vivo* model of Alzheimer's disease.[8] Regardless of this therapeutic effectiveness, clinical use of rapamycin is restricted by its low water solubility (~2.6 µg/mL), low stability of the active lactone in plasma and the pH range of 2–10, low bioavailability of oral formulations (~14%) and high affinity to red blood cells. Moreover, the unwanted immunosuppressive effect of rapamycin is an important issue that should be avoided in mentioned treatments.

Among different strategies for CNS drug delivery, as mentioned above, a brain-targeted nanocarrier could be a proper formulation for drugs to cross the BBB. In this study in order to design an efficient brain targeted delivery system for rapamycin and to reduce the immunosuppressive adverse effect of a drug, transferrin (Tf) decorated nanostructured lipid carriers (NLCs) were selected. The lipid core of NLCs, a mixture of solid and liquid lipids, incorporates the lipophilic rapamycin, protects the lactone ring from chemical and enzymatic degradation, increases the entrapment of drug, and prevents the loss of drug during brain targeting and the shelf-life period. On the other hand, the use of transferrin as a targeting moiety on the surface of NLCs facilitates transport across the BBB by binding to the transferrin receptors placed on the surface of the microvascular endothelial cells. Overexpression of transferrin receptor on the surface of glioblastoma tumor cells also resulted in dual targeting of transferrin decorated NLCs for this type of cancer.

This research aimed to prepare and optimize rapamycin-loaded NLCs with the previously selected lipids in the size below 150 nm by a simple solvent diffusion and sonication method and to decorate the optimized NLCs with transferrin by physical adsorption, as a mean of targeted brain delivery system. Additionally, *in vitro* cell viability, cellular uptake, and receptor-dependent uptake of transferrin decorated NLCs were evaluated on the U-87 MG glioblastoma cell line. Then the brain biodistribution and immunosuppressive effect of nanocarriers were also *in vivo*.

Materials and Methods

Materials

Rapamycin (Rapa) was provided from Polio (Lazio, Italy). Precirol ATO5 and capryol PGMC (propylene glycol monocaprylate) were kindly donated by Gattefossé (Lyon, France). Stearylamine (SA), human holo transferrin (Tf), and coumarin-6 (C6) were supplied from Santa Cruz (Mississauga, Canada). Tween 80, poloxamer 188, and 3- (4, 5-Dimethylthiazol-2-yl)-2, 5-diphenyltetrazolium bromide (MTT) were from Merck (Darmstadt, Germany).U-87 MG cell line was obtained from Pasteur Institute (Tehran, Iran). Dulbecco's Modified Eagle Medium (DMEM), Penicillin, streptomycin, fetal bovine serum (FBS), and trypsin were from Capricorn scientific (Frankfurt, Germany). All other chemicals were in pharmaceutical grade and received from commercial sources. Distilled and deionized water was used throughout.

Formulation process

According to our previously reported study, Precirol ATO5 and Capryol PGMC were selected as solid and liquid lipids respectively.[11] Cationic-NLCs (C-NLCs), containing SA as cationic lipid, were prepared by emulsification solvent diffusion-evaporation method the following ultrasonication. Briefly, Precirol ATO5, SA, Capryol PGMC, and rapamycin were dissolved in ethanol at 50°C and dispersed in the aqueous surfactant solution at 50°C using a magnetic stirrer at 1000 rpm. The resulting microemulsion was then ultrasonicated using a probe sonicator (Misonix S4000-010, USA) at 15 W powers and 50°C. The nanoemulsion was then cooled down in an ice bath and then was stirred (600 rpm) overnight at room temperature. Different formulations (presented in Table 1) for C-NLCs were prepared by varying the formulation and process variables to optimize the nanoparticle characterizations. To prepare bare NLCs (B-NLC), the optimum formulation of C-NLCs was used while Precirol was replaced with stearylamine.

NLCs characterization

The particle size, polydispersity index (PDI) and zeta potential of NLCs were measured by Zetasizer (Nano-ZS, Malvern, UK) at 25°C. The morphology of the optimized NLCs was evaluated by scanning electron microscopy (Philips, Eindhoven, the Netherland) and transmission electron microscopy (Zeiss, Jena, Germany).

Encapsulation efficiency & drug loading

The percentage of drug entrapment efficiency (EE %) and drug loading (DL %) were evaluated through an indirect method measuring unloaded drugs in the reaction medium. Briefly, the dispersion of prepared nanoparticles was centrifuged at 44720 rcf for 1 hour at 4°C and the amount of free drug in the supernatant was measured by reverse-phase high-pressure liquid chromatography (HPLC; Knauer, Berlin, Germany). The parameters were UV detector (K2600; Knauer, Berlin, Germany), C8 (MN, 15 × 4.6 mm, 5 µm particle size) HPLC column, mobile phase methanol:water (28:72 % v/v), the temperature at

Table 1. Formulation design of cationic-NLCs based on different formulation and process variables

Variables	Surfactant ratio (tween 80:poloxamer 188) with total concentration of 1% (w/v)	Lipid concentration %(w/v)	Solid lipid: liquid lipid	Sonication time (min)	Drug concentration (w/w)
Surfactant ratio	1:0, 3:1, 1.5:1 and 1:1	1	3:1	2	5
Lipid concentration	3:1	0.25, 0.5, 1, 3 and 5	3:1	2	5
Solid lipid: liquid lipid	3:1	1	6:1, 3:1 and 1.5:1	2	5
Sonication time	3:1	1	1.5:1	1, 2, 5, 7 and 10	5
Drug concentration	3:1	1	1.5:1	5	0, 5, 10 and 20

50°C, the flow rate at 1 mL/min and UV absorbance at 278 nm. EE% and DL% of rapamycin in nanoparticles were calculated by the following equations:

$$\%EE = \frac{Drug_{Total} - Drug_{Free}}{Drug_{Total}} \times 100$$

$$\%DL = \frac{Drug_{Total} - Drug_{Free}}{Nanoparticles\ weight} \times 100$$

Decoration of C-NLCs with transferrin

The Tf was physically decorated on the surface of C-NLCs via electrostatic interaction of the free carboxyl group of Tf with the amine group of stearylamine. Tf was dissolved in phosphate buffer saline (PBS) (pH 7.4) at a concentration of 1 mg/mL and was added to the C-NLCs suspension at a ratio of 1:1(w/w). The adsorption reaction was left for 24 hours. The free uncoupled Tf was removed using centrifugal filter tubes (Amicon Ultra, 100 kDa).

Determination of coupling efficiency

The amount of Tf adsorbed on the surface of the C-NLCs was determined by an indirect method. In this manner, the free uncoupled Tf was removed using centrifugal filter tubes (Amicon Ultra, 100 kDa). To determine the free Tf concentration the Bradford protein macro assay was applied using Coomassie blue G dye (Bradford 1976).[12] Coupling efficiency was expressed as mg Tf per mmol stearylamine.

Cell viability assay

Human glioblastoma-astrocytoma cells, U-87 MG, were grown in DMEM high glucose medium supplemented with 10% FBS, 2 mM L-glutamine, 100 U/mL penicillin, and 100 mg/mL streptomycin at 37°C in 5%CO_2. The effect of bare NLC (B-NLC), cationic NLC (C-NLC) and transferrin decorated NLC (Tf-NLC) on U-87 MG cell viability was evaluated by the MTT assay method. U-87 MG cells with a density of 10^4 cells/well were seeded in a 96-wells plate for 24 hours. Afterward, cells were treated with nanoparticles at concentrations of 0.01, 0.1, 1, 10, 100 µg/mL. After 24 h incubation, all samples were incubated with MTT (0.5 mg/mL) for 2 hours at 37°C. The formazan crystals were dissolved by 150 µL dimethylsulfoxide (DMSO). The optical density of samples was read by a plate reader at 570 nm (Tecan, Männedorf, Switzerland). Cell viability was demonstrated using the equation bellow[13]:

$$\%\ Cell\ viability = \frac{Optical\ density\ of\ nanoparticle\ treated\ cells}{Optical\ density\ of\ untreated\ cells\ (control)} \times 100$$

Cellular uptake assay

Confocal microscopy

The cellular uptake of coumarin-6 (C6) loaded B-NLC, C-NLC, and Tf-NLC by U-87 MG cells was studied using a confocal laser scanning microscopy (Nikon, Tokyo, Japan). Briefly, the C6 loaded nanoparticles were similarly prepared while C6 was replaced with rapamycin. U-87 MG cells (5×10^4 cells/well) were seeded on the coverslip in 6 well plates and incubated for 24 hours. After that, cells were treated with 1 µg/mL of different nanoparticles and incubated for 2 hours followed by treating by 1 mL of DAPI for 5 minutes. Finally, the cellular uptake of nanoparticles was evaluated by confocal laser microscopy.

Flow cytometry analysis

The uptake of nanoparticles by U-87 MG cells was also quantified through flow cytometry. Cells were seeded in a 6-well plate (10^5 cells/well) in DMEM medium with 10% FBS for 24 hours. Then cells were treated with C6 loaded B-NLC, C-NLC, and Tf-NLC and were incubated for 0.5, 1 and 2 hours at 37°C. To investigate the effect of protein corona on Tf-NLC cell uptake, cells were cultured in a serum-free medium. Furthermore, to evaluate the transferrin receptor-dependent cell uptake in Tf-NLC, cells were pre-incubated for 1 hour with transferrin solution at 200 µg/mL in order to saturate the Tf receptors. After treatment, cells were washed, detached from each well, and resuspended in PBS. The percentage of cellular uptake was evaluated by flow cytometer and analyzed by FlowJo software (FlowJo 10.0.9).

Biodistribution study

The biodistribution of nanoparticles was studied by coumarin-6 (C6) fluorescent dye on male mice weighing 30-40 g. C6 loaded B-NLC and Tf-NLC were injected into the tail vein of mice (5 mg C6/kg). Images were taken at different time points by the small animal *in vivo*

optical imaging (Fluovision, Iran) and were analyzed quantitatively by ImageJ (1.8.0) software. Radiographic image of mice with X-ray was also performed by Micro-Computed Tomography (Micro-CT) (LOTUS-inVivo, Tehran, Iran) to determine the exact location of the fluorescent dye accumulation. The animal tests were done according to the guidelines of the Animal Care and Ethics Committee of Tehran University of Medical Sciences.

WBC differential count

The effect of rapamycin-loaded NLCs on the immune system was studied by a differential count of white blood cells (WBC) of a rat. In this way, 24 male Wistar rats (200–250 g) were randomly divided into 4 groups and received IV injection of 1) saline (control group), 2) rapamycin solution (Rapa solution group), 3) rapamycin loaded B-NLCs (Rapa-B-NLC group) and 4) rapamycin loaded Tf-NLCs (Rapa-Tf-NLC group) respectively. In drug-treated groups, equivalent doses of 3.5 mg/kg rapamycin were used. Each animal received one injection/day for 6 consecutive days. Blood samples were collected 25 days after the first injection. WBC differential count was performed via a Hematology analyzer (MindrayBC-5000, Guangzhou, China).

All animal tests were done according to the guidelines of the Animal Care and Ethics Committee of Tehran University of Medical Sciences.

Statistical analysis

The results achieved from the experiments were statistically analyzed using Prism (GraphPad Prism 8.0.2). Multiple sample comparison was conducted via one-way ANOVA or two-way ANOVA according to the data set. A P-value less than 0.05 was considered significant. The results were presented as mean ± standard deviation (SD).

Results

According to our previous research, Precirol ATO5 and Capryol PGMC with the highest rapamycin solubility capacity were selected respectively as solid and liquid lipid ingredients of NLCs (11). For the preparation of C-NLCs the solvent diffusion–ultrasonication method was used. Effect of different formulation and process variables on size, PDI, ZP, and %EE are discussed in the following sections and is presented in Table 2.

Surfactants ratio

C-NLCs stabilized with Tween 80 (1% w/v) showed lower particle size (~170 nm) with broader PDI ~0.4. Adding Poloxamer 188 to the formulations led to a slight enlargement of the particles with a lower PDI. The best result was seen in formulation consisting of tween 80: poloxamer 188 (3:1 w/w) with a particle size of ~185 nm and PDI ~0.2.

Table 2. The physical characteristics of different cationic NLCs

Variables		Particle size (nm)	PDI	Zeta potential (mV)	EE%
Surfactant ratio (total concentration 1 %w/v)	Tween 80	174 ± 21	0.445 ± 0.012	21.6 ± 0.3	-
	Tween 80: Poloxamer188 (3:1)	185 ± 25	0.245 ± 0.012	20.4 ± 0.2	-
	Tween 80: Poloxamer188 (1.5:1)	195 ± 12	0.345 ± 0.043	20.1 ± 0.3	-
	Tween 80: Poloxamer188 (1:1)	224 ± 4	0.285 ± 0.052	19.9 ± 0.2	-
Lipid concentration (% w/v)	0.25	135 ± 21	0.563 ± 0.021	19.6 ± 1.8	-
	0.5	140 ± 18	0.405 ± 0.012	19.8 ± 2.1	-
	1	145 ± 12	0.326 ± 0.018	20.1 ± 1.6	-
	3	361 ± 8	0.254 ± 0.015	16.2 ± 2.3	-
	5	442 ± 9	0.263 ± 0.014	15.4 ± 1.8	-
Liquid lipid:Solid lipids	(6:1)	289 ± 12	0.37 ± 0.03	21.5 ± 0.7	82.2 ± 0.7
	(3:1)	209 ± 15	0.3 ± 0.08	20.9 ± 0.5	88.1 ± 0.8
	(1.5:1)	122 ± 13	0.342 ± 0.05	20.5 ± 0.6	94.4 ± 0.5
Drug concentration(%w/w)	0	192 ± 11	0.39 ± 0.05	19.5 ± 0.12	-
	5	159 ± 8	0.37 ± 0.03	20.7 ± 1.1	95.6 ± 1.1
	10	150 ± 15	0.402 ± 0.03	19.5 ± 1.4	94.3 ± 0.8
	20	143 ± 9	0.327 ± 0.04	20.1 ± 1.5	95.1 ± 0.5
Sonication time (min)	1	312 ± 5	0.257 ± 0.011	22 ± 0.7	-
	2	281 ± 7	0.205 ± 0.052	21.5 ± 0.8	-
	5	201 ± 4	0.218 ± 0.041	19.4 ± 0.9	-
	7	244 ± 4	0.381 ± 0.033	22.1 ± 0.1	-
	10	240 ± 11	0.414 ± 0.025	23 ± 0.11	-

Data as mean ± SD (n=3).
PDI: Polydispersity index. EE: Entrapment efficiency.

Lipid concentration

It was shown that increasing the lipid concentration (LC) from 0.25 to 5 % (w/v) significantly increased the particle size of nanoparticles (Table 2). C-NLCs with 0.25% (w/v) LC showed the lowest particle size and broader PDI. On the other hand, C-NLCs with 5% (w/v) LC showed the highest size and lowest PDI. ZP decreased by increasing the LC which is due to a fixed amount of stearylamine, as a cationic lipid, in this formulation. With 1% (w/v) LC, the optimum particle size, PDI and ZP were observed.

Solid lipid to liquid lipid ratio

As shown in Table 2, the particle size of prepared nanoparticles was decreased and reached a lower size (about 209 nm) by reducing the ratios of applied solid lipid and liquid lipid in nanoparticles. As can be seen, the %EE of nanoparticles increased from 80% to 94% by decreasing the mentioned ratio. Zeta potential of all formulations was about +20 mV as the amount of cationic solid lipid, stearylamine, was fixed in these formulations, and changing the concentration of the different lipids did not affect the surface charge of C-NLCs.

Sonication time

As shown in Table 2, the particle size decreased with increasing the sonication time from 1 to 5 minutes. An additional increase in sonication time (7 to 10 minutes) resulted in increased particle size.

Drug concentration

Among different formulations prepared with drug concentrations from 5% to 20%, there was no significant difference in particle size. But, between the empty and drug-loaded C-NLCs a size reduction was observed (Table 2). The ZP for obtained particles was approximately +20 mV, and no trend was found in surface charge by increasing the drug concentration. %EE for this range of drug content was more than 90% which represents the high capacity of nanoparticles for entrapment of rapamycin.

Characterization of optimized NLCs

From the results discussed above, the optimized formulation for rapamycin loaded NLCs was prepared as follows: Surfactants ratio = 3:1 (tween 80: poloxamer188), lipid concentration = 1% (w/v), solid lipid to liquid lipid ratio = 1.5:1, drug concentration = 20% (w/w) and sonication time = 5minutes. As shown in Table 3 the optimized NLCs showed low particle size, narrow PDI, and high %EE and %DL. Fig. 1C also showed the distribution patterns of particle size intensity and zeta potential of optimized C-NLCs. The results also demonstrated that following 24 hours incubation of C-NLCs with Tf solution there was a reduction in ZP (from ~ +22 to +3) and a slight increase in particle size which could indicate the physical adsorption of Tf.

The shape and surface morphology of rapamycin-loaded NLCs were also evaluated by SEM and TEM. Smooth surface morphology and spherical shape of the NLCs were observed by SEM imaging (Fig.. 1A). TEM analysis also showed a round shape and uniform distribution of nanoparticles (Fig. 1B).

The binding efficiency of Tf protein to C-NLCs, demonstrated by Bradford assay, was 25 ± 5 mg Tf per mmol of stearylamine.

Cell viability study

Fig. 2 shows the percentage survival of U-87MG cells after 24 hours exposure to different types of NLCs in the defined range of concentration. B-NLCs showed no toxicity in all studied concentrations. C-NLCs and Tf-NLCs exhibited more than 80% cell viability at concentration ≤1 µg/mL. But at higher concentrations, they showed significant cytotoxicity compared to B-NLCs. It should be noted that C-NLCs at concentration ≥1 µg/mL were significantly more toxic than Tf-NLCs. Thus, for further *in vitro* studies, the concentration of 1 µg/mL of different nanoparticles was selected.

Cellular uptake study

The confocal images for the cellular uptake of B-NLCs, C-NLCs, and Tf-NLCs, after 2 hours incubation, have been illustrated in Fig. 3A. As seems, the cellular accumulation of C-NLCs and Tf-NLCs was obviously higher than B-NLCs according to more green regions in the cytoplasm. These findings were also confirmed by flow cytometry analysis (Fig. 3B) in which the cell uptake percentage of both C-NLCs and Tf-NLCs were higher than B-NLCs at each time point and were statistically significant at 1 and 2 hours ($P < 0.001$). Further, pre-incubation of cells with excess Tf which resulted in the occupation of TfRs, reduced the Tf-NLCs cellular uptake at 1 and 2 hours ($P < 0.05$). Additionally, the cellular uptake of Tf-NLCs was reduced to a level similar to B-NLCs. Next, cellular uptake study of Tf-NLCs in serum-free media revealed a significantly

Table 3. The Characterization of optimized bare-NLCs (B-NLC), cationic-NLCs (C-NLC), and transferrin decorated NLCs (Tf-NLC) formulations

NLCs	Particle size (nm)	PDI	Zeta potential (mV)	EE%	DL%
B-NLC	127 ± 14	0.31 ± 0.02	(-10) ± 2.1	95.3 ± 1.1	13.8 ± 0.86
C-NLC	131 ± 10	0.19 ± 0.08	(+22) ± 2.5	96 ± 0.7	14.2 ± 0.66
Tf-NLC	149 ± 8	0.28 ± 0.06	(+3) ± 1.5	93.4 ± 1.5	13.5 ± 0.91

Data as mean±S.D (n=3).

PDI: Polydispersity index. EE: Entrapment efficiency. DL: Drug loading

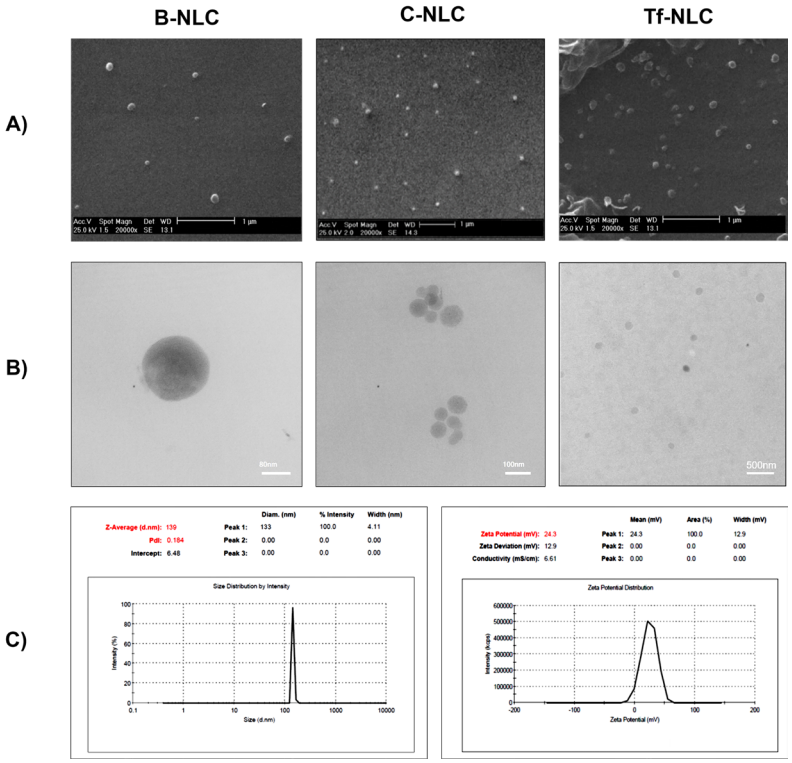

Fig. 1. Characterization of rapamycin-loaded bare NLCs (B-NLC), cationic NLCs (C-NLC), and transferrin decorated NLCs (Tf-NLC). (A) Scanning electron microscope photographs of different NLCs. (B) Transmission electron microscope photograph of different NLCs. (C) Particle size intensity and zeta potential distribution patterns of optimized C-NLCs.

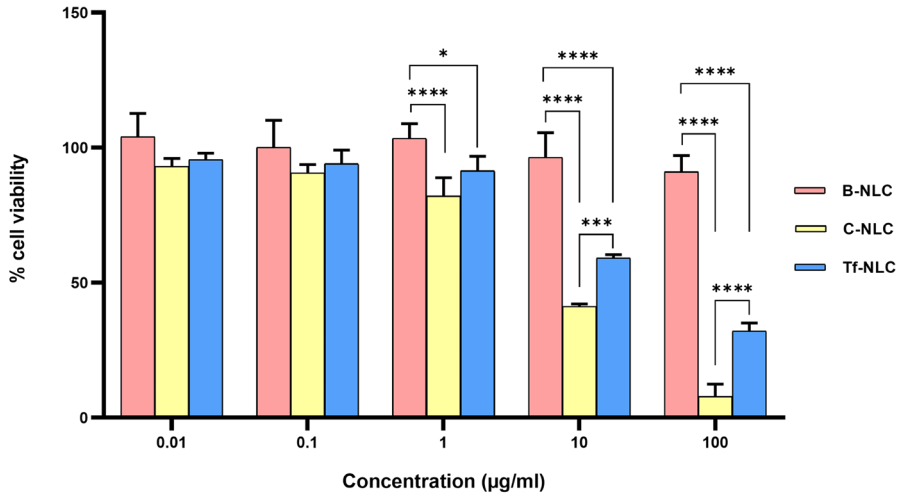

Fig. 2. Percent of viable U-87MG cells determined by MTT assay after 24 h incubation with bare NLC (B-NLC), cationic NLC (C-NLC), and transferrin decorated NLC (Tf-NLC) at different concentrations. Data are shown as mean ± SD. (*$P < 0.05$, ***$P < 0.001$, ****$P < 0.0001$). NLCs: Nanostructured lipid carriers.

higher uptake of Tf-NLCs at 0.5 ($P < 0.001$) and 1 hour ($P < 0.05$) in comparison to serum-based media which demonstrated an increased rate in Tf-NLCs uptake, but finally after 2 hours the extent of Tf-NLCs cellular uptake was same in serum-based and serum-free media (Fig. 3B).

Based on confocal images and flow cytometry data, shown in Fig. 3 there was no difference between C-NLCs and Tf-NLCs cell uptake in all studied incubation times.

Biodistribution study

Fig. 4A shows the fluorescent images of mice after IV injection of coumarin-6 (C6) loaded B-NLCs and Tf-NLCs. According to the *in vitro* cell viability assay, as the C-NLCs showed great toxicity in a concentration higher than 1 µg/mL, for ethical consideration this group was omitted from fluorescent imaging studies. The imaging was done at different time points up to 24h to follow the

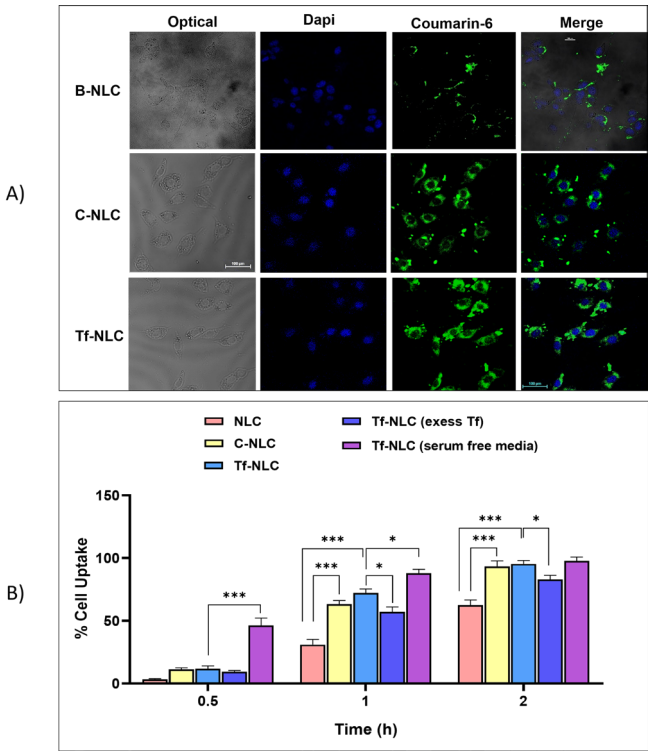

Fig. 3. Cellular uptake of different types of NLCs on U-87MG cells. (A) Confocal images for cellular uptake of coumarin-6 loaded bare NLCs (B-NLC), cationic NLCs (C-NLC) and transferrin decorated NLCs (Tf-NLC) after 2hours incubation. (B) Percentages of cellular uptake of coumarin-6 loaded bare NLCs (B-NLC), cationic NLCs (C-NLC), and transferrin decorated NLCs (Tf-NLC) (with and without serum, and 1 h pre-incubation with excess free Tf) after 0.5, 1 and 2 hours incubation at 37ºC, determined by flow cytometry. Data are shown as mean±SD. (*P<0.05, ***P<0.001). NLCs: Nanostructured lipid carriers.

distribution pattern of nanoparticles. The quantitative analysis of fluorescent intensity in brain and lung areas and also the brain/lung ratio are shown in Fig. 4C based on the region of interest determined in X-ray imaging of mice (Fig. 4B).

In both B-NLCs and Tf-NLCs groups, the fluorescent emissions were detected in the brain area at 1h which was greater for Tf-NLCs group as a targeted delivery system. Further, B-NLCs showed the maximum brain accumulation after 3h and then a decrease in the intensity at 6h which was stable up to 24 hours. But then for Tf-NLCs group there was an increasing trend in fluorescent intensity up to 6 hours in the brain area which was steady up to 24 hours. These results confirmed the brain accumulation of both nanoparticles but, unexpectedly, from the quantitative analysis the brain fluorescent intensity in B-NLCs group was more than TF-NLCs group at 3 hours. A study of the fluorescence dye accumulation in the lung area also showed a higher level with an increasing trend for B-NLCs group, while for Tf-NLCs group, low and constant pulmonary accumulation was recorded. The brain/lung ratio of fluorescent intensity in these two groups showed higher targeted accumulation for Tf-NLCs.

Effect on the immune system

Fig. 5 shows the differential white blood cell (WBC) count in experimental groups. In the Rapa solution group the lymphocyte count significantly decreased (P<0.0001) compare to the control group which demonstrated the immunosuppressive effect of rapamycin. On the other hand, the neutrophil count significantly increased (P<0.0001) in comparison to the control group which is related to a possible infection following the weakened immune system. However, remarkably, in both Rapa-B-NLC and Rapa-Tf-NLC groups, the immunosuppressive effect of rapamycin was not seen and the lymphocyte and neutrophil counts of animals were statistically equal to the control group.

Discussion

Therapeutic potential of rapamycin as an mTOR inhibitor is reported in numerous researches for brain-related diseases especially glioblastoma[14,15] and neurodegenerative diseases.[8,16,17] However, the clinical use of rapamycin for CNS related diseases is restricted due to very low oral bioavailability, chemical and enzymatic degradation limited BBB transport and undesirable immunosuppressive effect.[18,19]

Considering all these issues, in order to design an efficient brain targeted delivery system for rapamycin and to overcome the above-mentioned drawbacks, transferrin decorated NLC for brain delivery of rapamycin was designed. Since rapamycin is a substrate for P-glycoprotein (p-gp) efflux pump on BBB, the use of Tf-NLCs can circumvent such drug efflux and increase the efficiency

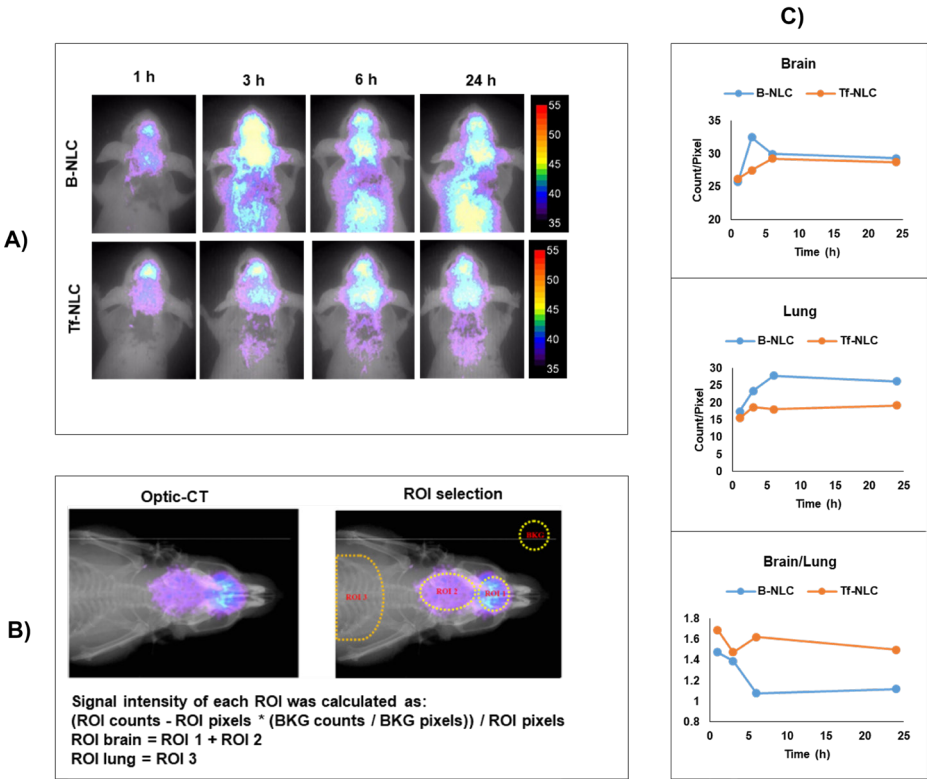

Fig. 4. Qualitative and quantitative biodistribution of coumarin-6 loaded bare NLC (B-NLC) and transferrin decorated NLC (Tf-NLC). (A) The fluorescent imaging of brain and lung areas of mice in different time points after tail vein injection of B-NLC and Tf-NLC. (B) The radiographic image of mice. (C) The quantitative graph of the brain and lung emitted fluorescence intensity by B-NLC and Tf-NLC. NLCs: Nanostructured lipid carriers.

of brain drug delivery by receptor-mediated transcytosis.[20] The main challenges related to the preparation of the nanostructures and their biological interactions with cells and the BBB were evaluated *in vitro* and *in vivo*.

As rapamycin is a heat-sensitive drug, in order to achieve a suitable particle size for brain delivery, herein, the solvent diffusion–ultrasonication method was found to be efficient and simple for the preparation of C-NLCs. According to our previous study, Precirol ATO5 and Capryol PGMC were selected respectively as solid and liquid lipid ingredients of NLCs.[11] Here stearylamine plays as a cationic lipid and creates a positive charge for physical adsorption of transferrin on the surface of NLCs through electrostatic interaction.

Precirol ATO 5, composed of, di- and triglycerides of palmitic and stearic acids, has been used in different studies in varying concentrations for the core matrix of lipid nanoparticles. Precirol could make small lipid nanoparticles with a narrow PDI and also offers acceptable lipophilicity to the NLCs which could increase brain delivery efficiency. Another hand, lipids with longer fatty acid chains, like Precirol, are less susceptible to enzymatic degradation which provides long-circulating properties to the carrier system in the blood.[21]

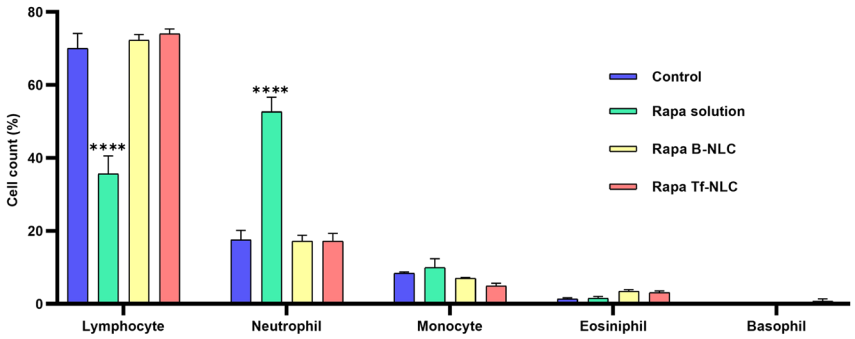

Fig. 5. Variation of WBC differential count in different treated groups. Data are shown as mean ± SEM (N = 6 rats in each group). Statistical analysis = one-way ANOVA post-test Tukey. (****P < 0.0001 significantly difference compared to control group). Rapa: Rapamycin; B-NLC: Bare NLC; Tf-NLC: Transferrin decorated NLC; NLC: Nanostructured lipid carriers.

The non-ionic surfactants, tween 80 and poloxamer 188 (total surfactant concentration 1%) were selected in the present study for stabilizing the NLCs and increasing the BBB permeability. The use of poloxamer 188 as a co-surfactant in combination with tween 80 could improve the stability of lipid nanoparticles. Tween 80 as a fatty acid-based surfactant offers considerable stability to the system due to the fatty acid chain integrated into the lipid matrix and the hydrophilic portion places outside in the aqueous phase. On the other hand, poloxamers 188 as a steric stabilizer adsorbs on the surface of the lipid matrix.[22] Furthermore, the addition of Poloxamer 188 to the formulation of lipid nanoparticles leads to a slight increase of the particle size whereas more stable formulations, which is similar to our results.[23] Hydrophilic-lipophilic balance (HLB) value of 12–16 is supposed to be an optimum value for the production of a stable o/w emulsion. Tween 80 with the HLB value of ~15 is within this range, however, the HLB value of poloxamer 188 is very high (~29). This might be the reason for the larger particle size obtained when poloxamer 188 was used in the formulations.

Lipid concentration (LC) showed a significant effect on the particle size of nanoparticles. It has been assumed that an increase in LC by increasing the lipid phase viscosity reduces the uniform distribution of sonication energy and therefore results in larger particle size.[24] Enhancing the viscosity of the lipid phase also reduces the diffusion rate of the solute molecules from lipid droplets and leads to larger particles. Additionally, increasing the concentration of the lipid phase can augment the collisions and aggregation of the nanoparticles.[25] However, as the surfactant concentration leaves constant, increasing the LC, enhances the lipid/surfactant ratio and thereby insufficient surfactant could not properly make protective layers on C-NLCs and resulted in particles aggregation.[26]

The solid lipid to liquid lipid ratio affects the particle size and %EE of NLCs. Reduction of this ratio resulted in lower particle size. This observation was also reported in other studied NLCs.[27] Additionally, the increase in %EE of C-NLCs by decreasing the mentioned ratio may be attributed to the high lipophilicity of rapamycin. The solubility of drugs in solid lipids is usually lower than liquid lipids, relating to the longer carbon chain in the solid lipids. Hence by increasing the liquid lipid fraction, the %EE increased. There is a structural difference between solid and liquid lipids. In the presence of liquid lipid, the solid lipid molecules cannot be arranged into a perfect crystalline structure during solidification and form amorphous or less crystalline structures. Therefore, the presence of the imperfections provides more space for the drug entrapment which is responsible for the higher %EE by increasing the liquid lipid fraction.

Sonication time showed an obvious effect on the particle size of C-NLCs. As the sonication process is the final step to produce nanoemulsion droplets from the microemulsion drops, extended sonication time (herein up to 5 minutes) by inducing higher sonication energy to the NLC dispersions decrease the size of nanoemulsion droplets. On the other hand, as the temperature of the medium was above the melting point of lipids through the sonication process facilitate the subdivision of oil droplets. Additional increase in sonication time enlarged the particle size which may be due to agglomeration of very fine droplets as a result of induced high surface energy. These observations were following previous reported researches.[28,29]

Change in drug concentration (DC) showed no significant difference in particle size but, a size reduction was seen between the empty and drug-loaded C-NLCs (Table 2) which was in agreement with other described studies.[30] This result may be attributed to the hydrophobic interaction of rapamycin with the lipid matrix leading to the condensation of particles and reduction in size. However, in our previous study as the drug concentration of nanoparticles was lower (2%), an increase in particle size was demonstrated in comparison to empty ones (216 ± 40 vs. 176 ± 25, respectively).[11] This lack in reduction of particle size in case of the lower level of drug may be related to the inadequate drug molecules for induction of high degree of hydrophobic interaction.

The optimized formulation of rapamycin-loaded C-NLCs and B-NLCs were prepared and showed low particle size and spherical shape with a high EE capacity.

The optimized C-NLCs were physically decorated with Tf. Physical adsorption of proteins on a charged solid surface is controlled by non-covalent binding forces mainly electrostatic attraction. The isoelectric point of Tf is around pH = 6.5 which above of this pH (i.e. pH = 7.4 in working solutions) exhibited a negative charge.[31] The positive zeta potential of the prepared C-NLCs (~+22 mV), mediated by the NH_3^+ group of stearylamine, enables the electrostatic attachment of negative charged Tf by the COO^- groups. It should be considered that there is a difference between the pH near the surface of a charged particle (pH_S) and the pH of the bulk solution (pH_B). So that the pH_S of a positive solid surface is more alkaline than pH_B.[32] This alkaline environment near the surface could make the Tf more negative which might further facilitate the electrostatic adsorption. The binding efficiency of Tf protein to C-NLCs was also in the middle range of other previous reports.[33,34]

Based on cell viability assay C-NLCs showed cytotoxicity in high concentrations which may be related to the positive charge of particles. Otherwise, as B-NLC and TF-NLC showed respectively no toxicity and moderate toxicity in high concentrations, it could be concluded that the observed toxicity may be also related to the molecule of stearylamine in nanoparticles. In this manner, studies also showed that single-tailed cationic surfactants are more toxic than double-tailed ones and their toxicity is probably concentration dependent.[33,35-37]

The cellular uptake of coumarin-6 loaded nanoparticles was studied both qualitatively and quantitatively by confocal microscopy and flow cytometry. Cell surfaces have a negative charge due to the presence of sulfated proteoglycans molecules in a lipid bilayer. Nanoparticles with a positive surface charge can bind strongly to the cell membrane and thus exhibited higher cellular uptake by adsorption-mediated endocytosis. U-87 MG cells present a high level of transferrin receptors (TfR).[38] Thereby, the high level of Tf-NLCs cellular uptake could be related to the specific Tf/TfR uptake. Further, the use of excess free Tf reduced the binding sites accessible for the Tf-NLCs and thereby inhibited the active receptor-mediated endocytosis process. This result confirmed the receptor-dependent uptake of Tf-NLCs. By this outcome, the receptor-dependent transcytosis of TF-NLCs by TfRs on BBB could also be expected. Moreover, it should be noted that in the presence of excess Tf, the cellular uptake of Tf-NLCs was reduced to a level similar to B-NLCs. As a result, the inhibitory effect of the excess free Tf confirmed the existence of additional endocytosis pathways for Tf-NLCs. Similar results were also reported by other researchers.[39] In addition, no significant difference between C-NLCs and Tf-NLCs cell uptake in all studied incubation times confirmed the difference in endocytosis mechanism.

Biodistribution study showed appropriate brain uptake of Tf-NLCs with low pulmonary uptake as an untargeted tissue. B-NLCs also presented high brain accumulation but the lung accumulation was also high. According to studies done in the field of the protein corona, after parenteral injection, nanoparticles with a coat of tween 80 could adsorb the plasma lipoproteins mainly ApoE. This adsorption can then induce the receptor-mediated transcytosis of nanoparticles across the BBB via low-density lipoprotein receptors. This process can be considered as a reason for the higher brain accumulation of B-NLCs particles.[40] On the other hand, the protein corona effect on Tf-NLCs could have some negative outcomes on the targeting property of Tf which could slow down the transferrin-dependent absorption in the targeted tissue.[41] Another limiting factor in brain accumulation of Tf-NLCs is the presence of high endogenous transferrin levels in plasma, which saturate the transferrin receptors in the BBB. Competition between nanoparticle-bound Tf and endogenous Tf to bind the receptor will reduce the rate and amount of brain accumulation of Tf decorated nanoparticles.[42] However, it should be also considered that there are some challenges in fluorescent imaging data, which is resulted in false positive or false negative results and is related to three phenomena including quenching, dequenching and saturation of dye.[43]

Yanez et al prepared Rapa loaded in PEG-block-poly (ε-caprolactone) (PEG-b-PCL) micelle formulations and demonstrated that the brain distribution of nanoparticles was considerably low.[44] Kadakia et al also fabricated fish oil-based nanoemulsion of Rapa for CNS drug delivery but they showed that this formulation was not successful for BBB penetration in mice.[45] Herein, our study showed that Tf-NLCs exhibited acceptable brain distribution with lower accumulation in the lung as a *reticuloendothelial system*.

Rapamycin is an immunosuppressive drug that has FDA approval for the prevention of organ transplant rejection, mainly in a kidney allograft. Rapamycin by making a complex with the 12-kDa FK506-binding protein (FKBP12) and inhibition of the mTORC1 blocks T and B lymphocyte proliferation by disruption of a cytokine signaling that stimulates lymphocyte growth and differentiation.[46] Herein, unlike the Rapa-solution which showed obvious immunosuppression, B-NLCs and Tf-NLCs showed no suppression on the immune system. These findings indicated the low systemic exposure of free rapamycin in NLCs groups which was related to the complete entrapment of the drug in the nanoparticles. In the use of rapamycin for therapeutic purposes other than weakening the immune system, reducing or eliminating this adverse effect is very important. In our study, the prepared rapamycin-loaded NLCs effectively abolished this adverse effect.

Research Highlights

What is the current knowledge?

√ Currently, rapamycin has shown multiple pharmacologic effects for brain-related diseases mainly glioblastoma and neurodegenerative disease.

√ Clinical use of rapamycin for the brain-related disease is restricted due to low oral bioavailability, rapid systemic degradation, and immunosuppressive adverse effect.

√ The application of lipid nanoparticles for the efficient brain delivery of drugs has involved wide attention.

What is new here?

√ Efficient transferrin (Tf) decorated nanostructured lipid carriers (NLCs) of rapamycin were successfully prepared and characterized.

√ Tf-NLCs in comparison to bare NLCs (B-NLCs) exhibited higher U-87 MG cellular uptake.

√ Both B-NLCs and Tf-NLCs indicated appropriate brain uptake but Tf-NLCs showed lower accumulation in the lung.

√ Both B-NLCs and Tf-NLCs showed no immunosuppressive effect.

Conclusion

In this study, rapamycin-loaded C-NLCs were successfully prepared by emulsification solvent diffusion-evaporation and ultrasonication method, and the optimum nanoparticles were coated physically with transferrin (Tf) for targeting the brain tissue and facilitating the BBB penetration. The rapamycin-loaded Tf-NLCs exhibited low particle size and high drug loading capacity. Tf-NLCs

showed high cellular uptake in a receptor-dependent manner, an appropriate distribution in the brain, lower accumulation in lung tissue, and no immunosuppressive effect. According to our findings, the rapamycin-loaded Tf-NLCs could be considered as a proper formulation for CNS delivery.

Acknowledgments
The authors acknowledge TUMS Preclinical Core Facility (TPCF) for providing facilities for animal optic imaging.

Funding sources
This work was supported by the Tehran University of Medical Sciences (#27626) and Nanotechnology Research Center (42066).

Ethical statement
The animals were treated according to the protocols evaluated and approved by the ethical committee of Tehran University of Medical Sciences. The authors state that they have obtained appropriate institutional review board approval (IR.TUMS.VCR.REC.1398.422) or have followed the principles outlined in the Declaration of Helsinki for all animal experimental investigations.

Competing interests
The authors declare there is no conflict of interest.

Authors' contribution
All authors contributed to the conception and design of the work. FK and MH contributed to the acquisition, analysis, and interpretation of data for the work. FK wrote the draft. RD, MS, and FA supervised all aspects of the work in ensuring that questions related to the accuracy or integrity of any part of the work are appropriately investigated and resolved. FA revised the work critically for important intellectual content and approved the final version to be published.

References

1. Barar J, Rafi MA, Pourseif MM, Omidi Y. Blood-brain barrier transport machineries and targeted therapy of brain diseases. *Bioimpacts* **2016**; 6: 225-48. https://doi.org/10.15171/bi.2016.30
2. Patel MM, Goyal BR, Bhadada SV, Bhatt JS, Amin AF. Getting into the brain: approaches to enhance brain drug delivery. *CNS Drugs* **2009**; 23: 35-58. https://doi.org/10.2165/0023210-200923010-00003
3. Manaspon C, Nasongkla N, Chaimongkolnukul K, Nittayacharn P, Vejjasilpa K, Kengkoom K, *et al.* Injectable SN-38-loaded Polymeric Depots for Cancer Chemotherapy of Glioblastoma Multiforme. *Pharm Res* **2016**; 33: 2891-903. https://doi.org/10.1007/s11095-016-2011-4
4. Mc Carthy DJ, Malhotra M, O'Mahony AM, Cryan JF, O'Driscoll CM. Nanoparticles and the blood-brain barrier: advancing from in-vitro models towards therapeutic significance. *Pharm Res* **2015**; 32: 1161-85. https://doi.org/10.1007/s11095-014-1545-6
5. Buse J, El-Aneed A. Properties, engineering and applications of lipid-based nanoparticle drug-delivery systems: current research and advances. *Nanomedicine (Lond)* **2010**; 5: 1237-60. https://doi.org/10.2217/nnm.10.107
6. Dos Santos Rodrigues B, Kanekiyo T, Singh J. ApoE-2 Brain-Targeted Gene Therapy Through Transferrin and Penetratin Tagged Liposomal Nanoparticles. *Pharm Res* **2019**; 36: 161. https://doi.org/10.1007/s11095-019-2691-7
7. Venishetty VK, Komuravelli R, Kuncha M, Sistla R, Diwan PV. Increased brain uptake of docetaxel and ketoconazole loaded folate-grafted solid lipid nanoparticles. *Nanomedicine* **2013**; 9: 111-21. https://doi.org/10.1016/j.nano.2012.03.003
8. Spilman P, Podlutskaya N, Hart MJ, Debnath J, Gorostiza O, Bredesen D, *et al.* Inhibition of mTOR by rapamycin abolishes cognitive deficits and reduces amyloid-beta levels in a mouse model of Alzheimer's disease. *PLoS One* **2010**; 5: e9979. https://doi.org/10.1371/journal.pone.0009979
9. Malagelada C, Jin ZH, Jackson-Lewis V, Przedborski S, Greene LA. Rapamycin Protects against Neuron Death in In Vitro andIn Vivo Models of Parkinson's Disease. *Journal of Neuroscience* **2010**; 30: 1166-75.
10. Iorio AL, Da Ros M. Combined Treatment with Doxorubicin and Rapamycin Is Effective against In Vitro and In Vivo Models of Human Glioblastoma. *J Clin Med* **2019**; 8: 33. https://doi.org/10.3390/jcm8030331
11. Zahir-Jouzdani F, Khonsari F, Soleimani M, Mahbod M, Arefian E, Heydari M, *et al.* Nanostructured lipid carriers containing rapamycin for prevention of corneal fibroblasts proliferation and haze propagation after burn injuries: In vitro and in vivo. *J Cell Physiol* **2019**; 234: 4702-12. https://doi.org/10.1002/jcp.27243
12. Bradford MM. A rapid and sensitive method for the quantitation of microgram quantities of protein utilizing the principle of protein-dye binding. *Anal Biochem* **1976**; 72: 248-54. https://doi.org/10.1006/abio.1976.9999
13. Gandomi N, Varshochian R, Atyabi F, Ghahremani MH, Sharifzadeh M, Amini M, *et al.* Solid lipid nanoparticles surface modified with anti-Contactin-2 or anti-Neurofascin for brain-targeted delivery of medicines. *Pharm Dev Technol* **2017**; 22: 426-35. https://doi.org/10.1080/10837450.2016.1226901
14. Cloughesy TF, Yoshimoto K, Nghiemphu P, Brown K, Dang J, Zhu S, *et al.* Antitumor activity of rapamycin in a Phase I trial for patients with recurrent PTEN-deficient glioblastoma. *PLoS Med* **2008**; 5: e8. https://doi.org/10.1371/journal.pmed.0050008
15. Arcella A, Biagioni F, Antonietta Oliva M, Bucci D, Frati A, Esposito V, *et al.* Rapamycin inhibits the growth of glioblastoma. *Brain Res* **2013**; 1495: 37-51. https://doi.org/10.1016/j.brainres.2012.11.044
16. Bove J, Martinez-Vicente M, Vila M. Fighting neurodegeneration with rapamycin: mechanistic insights. *Nat Rev Neurosci* **2011**; 12: 437-52. https://doi.org/10.1038/nrn3068
17. Pan T, Kondo S, Zhu W, Xie W, Jankovic J, Le W. Neuroprotection of rapamycin in lactacystin-induced neurodegeneration via autophagy enhancement. *Neurobiol Dis* **2008**; 32: 16-25. https://doi.org/10.1016/j.nbd.2008.06.003
18. Polchi A, Magini A, Mazuryk J, Tancini B, Gapinski J, Patkowski A, *et al.* Rapamycin Loaded Solid Lipid Nanoparticles as a New Tool to Deliver mTOR Inhibitors: Formulation and in Vitro Characterization. *Nanomaterials (Basel)* **2016**; 6: 87. https://doi.org/10.3390/nano6050087
19. Abraham RT, Wiederrecht GJ. Immunopharmacology of rapamycin. *Annu Rev Immunol* **1996**; 14: 483-510. https://doi.org/10.1146/annurev.immunol.14.1.483
20. Benet LZ, Cummins CL. The drug efflux-metabolism alliance: biochemical aspects. *Adv Drug Deliv Rev* **2001**; 50 Suppl 1: S3-11. https://doi.org/10.1016/s0169-409x(01)00178-8
21. Müller RH, Rühl D, Runge SA. Biodegradation of solid lipid nanoparticles as a function of lipase incubation time. *International Journal of Pharmaceutics* **1996**; 144: 115-21. https://doi.org/10.1016/S0378-5173(96)04731-X
22. Patel K, Padhye S, Nagarsenker M. Duloxetine HCl lipid nanoparticles: preparation, characterization, and dosage form design. *AAPS PharmSciTech* **2012**; 13: 125-33. https://doi.org/10.1208/s12249-011-9727-6
23. Aboutaleb E, Noori M, Gandomi N, Atyabi F, Fazeli MR, Jamalifar H, *et al.* Improved antimycobacterial activity of rifampin using solid lipid nanoparticles. *Int Nano Lett* **2012**; 2: 33. https://doi.org/10.1186/2228-5326-2-33
24. Pradhan M, Singh D, Singh MR. Influence of selected variables on fabrication of Triamcinolone acetonide loaded solid lipid nanoparticles for topical treatment of dermal disorders. *Artif Cells Nanomed Biotechnol* **2016**; 44: 392-400. https://doi.org/10.3109/21691401.2014.955105
25. Hejri A, Khosravi A, Gharanjig K, Hejazi M. Optimisation of the formulation of beta-carotene loaded nanostructured lipid carriers prepared by solvent diffusion method. *Food Chem* **2013**; 141: 117-

23. https://doi.org/10.1016/j.foodchem.2013.02.080
26. Kumar R, Yasir M, Saraf SA, Gaur PK, Kumar Y, Singh AP. Glyceryl monostearate based nanoparticles of mefenamic acid: Fabrication and in vitro characterization. *Drug Invention Today* **2013**; 5: 246-50. https://doi.org/10.1016/j.dit.2013.06.011
27. Song A, Zhang X, Li Y, Mao X, Han F. Effect of liquid-to-solid lipid ratio on characterizations of flurbiprofen-loaded solid lipid nanoparticles (SLNs) and nanostructured lipid carriers (NLCs) for transdermal administration. *Drug Dev Ind Pharm* **2016**; 42: 1308-14. https://doi.org/10.3109/03639045.2015.1132226
28. Jain S, Chourasia M, Masuriha R, Soni V, Jain A, Jain NK, *et al.* Solid lipid nanoparticles bearing flurbiprofen for transdermal delivery. *Drug Delivery* **2005**; 12: 207-15.
29. Siddiqui A, Alayoubi A, El-Malah Y, Nazzal S. Modeling the effect of sonication parameters on size and dispersion temperature of solid lipid nanoparticles (SLNs) by response surface methodology (RSM). *Pharm Dev Technol* **2014**; 19: 342-6. https://doi.org/10.3109/10837450.2013.784336
30. Padamwar MN, Pokharkar VB. Development of vitamin loaded topical liposomal formulation using factorial design approach: Drug deposition and stability. *Int J Pharm* **2006**; 320: 37-44. https://doi.org/10.1016/j.ijpharm.2006.04.001
31. Eltayeb SE, Su Z, Shi Y, Li S, Xiao Y, Ping Q. Preparation and optimization of transferrin-modified-artemether lipid nanospheres based on the orthogonal design of emulsion formulation and physically electrostatic adsorption. *Int J Pharm* **2013**; 452: 321-32. https://doi.org/10.1016/j.ijpharm.2013.05.019
32. Aramesh M, Shimoni O, Ostrikov K, Prawer S, Cervenka J. Surface charge effects in protein adsorption on nanodiamonds. *Nanoscale* **2015**; 7: 5726-36. https://doi.org/10.1039/c5nr00250h
33. Khajavinia A, Varshosaz J, Dehkordi AJ. Targeting etoposide to acute myelogenous leukaemia cells using nanostructured lipid carriers coated with transferrin. *Nanotechnology* **2012**; 23: 405101. https://doi.org/10.1088/0957-4484/23/40/405101
34. Mulik RS, Monkkonen J, Juvonen RO, Mahadik KR, Paradkar AR. Transferrin mediated solid lipid nanoparticles containing curcumin: enhanced in vitro anticancer activity by induction of apoptosis. *Int J Pharm* **2010**; 398: 190-203. https://doi.org/10.1016/j.ijpharm.2010.07.021
35. Tabatt K, Sameti M, Olbrich C, Müller RH, Lehr C-M. Effect of cationic lipid and matrix lipid composition on solid lipid nanoparticle-mediated gene transfer. *Eur J Pharm Biopharm* **2004**; 57: 155-62. https://doi.org/10.1016/j.ejpb.2003.10.015
36. De M, Ghosh S, Sen T, Shadab M, Banerjee I, Basu S, *et al.* A Novel Therapeutic Strategy for Cancer Using Phosphatidylserine Targeting Stearylamine-Bearing Cationic Liposomes. *Mol Ther Nucleic Acids* **2018**; 10: 9-27. https://doi.org/10.1016/j.omtn.2017.10.019
37. Sharma S, Rajendran V, Kulshreshtha R, Ghosh PC. Enhanced efficacy of anti-miR-191 delivery through stearylamine liposome formulation for the treatment of breast cancer cells. *Int J Pharm* **2017**; 530: 387-400. https://doi.org/10.1016/j.ijpharm.2017.07.079
38. Anonymous. **2019**; Available from: https://www.proteinatlas.org/ENSG00000072274-TFRC/cell.
39. Gan CW, Feng SS. Transferrin-conjugated nanoparticles of poly(lactide)-D-alpha-tocopheryl polyethylene glycol succinate diblock copolymer for targeted drug delivery across the blood-brain barrier. *Biomaterials* **2010**; 31: 7748-57. https://doi.org/10.1016/j.biomaterials.2010.06.053
40. Azhari H, Strauss M, Hook S, Boyd BJ, Rizwan SB. Stabilising cubosomes with Tween 80 as a step towards targeting lipid nanocarriers to the blood–brain barrier. *Eur J Pharm Biopharm* **2016**; 104: 148-55. https://doi.org/10.1016/j.ejpb.2016.05.001
41. Pitek AS, O'Connell D, Mahon E, Monopoli MP, Baldelli Bombelli F, Dawson KA. Transferrin coated nanoparticles: study of the bionano interface in human plasma. *PLoS One* **2012**; 7: e40685. https://doi.org/10.1371/journal.pone.0040685
42. Paterson J, Webster CI. Exploiting transferrin receptor for delivering drugs across the blood-brain barrier. *Drug Discov Today Technol* **2016**; 20: 49-52. https://doi.org/10.1016/j.ddtec.2016.07.009
43. Meng F, Wang J, Ping Q, Yeo Y. Quantitative Assessment of Nanoparticle Biodistribution by Fluorescence Imaging, Revisited. *ACS nano* **2018**; 12: 6458-68. https://doi.org/10.1021/acsnano.8b02881
44. Yanez JA, Forrest ML, Ohgami Y, Kwon GS, Davies NM. Pharmacometrics and delivery of novel nanoformulated PEG-b-poly(epsilon-caprolactone) micelles of rapamycin. *Cancer Chemother Pharmacol* **2008**; 61: 133-44. https://doi.org/10.1007/s00280-007-0458-z
45. Kadakia E, Harpude P, Parayath N, Bottino D, Amiji M. Challenging the CNS Targeting Potential of Systemically Administered Nanoemulsion Delivery Systems: a Case Study with Rapamycin-Containing Fish Oil Nanoemulsions in Mice. *Pharm Res* **2019**; 36: 134. https://doi.org/10.1007/s11095-019-2667-7
46. Dumont FJ, Su Q. Mechanism of action of the immunosuppressant rapamycin. *Life Sci* **1996**; 58: 373-95. https://doi.org/10.1016/0024-3205(95)02233-3